**Defense Threat Reduction Agency**
**8725 John J. Kingman Road, MS-6201**
**Fort Belvoir, VA 22060-6201**

**DTRA-TR-14-42**

TECHNICAL REPORT

# Encapsulated Fluorescent Ag NPs as Novel Indicators for High-Energy Ionizing Radiation

Approved for public release; distribution is unlimited.

June 2014

MIPR 10-2650M

Dr. Scott A. Trammell and
Dr. Brett Martin

Prepared by:
Center for Bio/Molecular
Science and Engineering
Code 6900
Naval Research Laboratory
Washington, DC 20375

**DESTRUCTION NOTICE:**

Destroy this report when it is no longer needed.
Do not return to sender.

PLEASE NOTIFY THE DEFENSE THREAT REDUCTION AGENCY, ATTN: DTRIAC/ J9STT, 8725 JOHN J. KINGMAN ROAD, MS-6201, FT BELVOIR, VA 22060-6201, IF YOUR ADDRESS IS INCORRECT, IF YOU WISH THAT IT BE DELETED FROM THE DISTRIBUTION LIST, OR IF THE ADDRESSEE IS NO LONGER EMPLOYED BY YOUR ORGANIZATION.

# REPORT DOCUMENTATION PAGE

*Form Approved*
*OMB No. 0704-0188*

Public reporting burden for this collection of information is estimated to average 1 hour per response, including the time for reviewing instructions, searching existing data sources, gathering and maintaining the data needed, and completing and reviewing this collection of information. Send comments regarding this burden estimate or any other aspect of this collection of information, including suggestions for reducing this burden to Department of Defense, Washington Headquarters Services, Directorate for Information Operations and Reports (0704-0188), 1215 Jefferson Davis Highway, Suite 1204, Arlington, VA 22202-4302. Respondents should be aware that notwithstanding any other provision of law, no person shall be subject to any penalty for failing to comply with a collection of information if it does not display a currently valid OMB control number. **PLEASE DO NOT RETURN YOUR FORM TO THE ABOVE ADDRESS.**

| **1. REPORT DATE** *(DD-MM-YYYY)* | **2. REPORT TYPE** | **3. DATES COVERED** *(From - To)* |
|---|---|---|
| 00-06-2014 | Technical | Sept. 1, 2010 - Sept. 1, 2013 |

**4. TITLE AND SUBTITLE**

Encapsulated Fluorescent Ag NPs as Novel Indicators for High-Energy Ionizing Radiation

**5a. CONTRACT NUMBER**
MIPR 10-2650M

**5b. GRANT NUMBER**

**5c. PROGRAM ELEMENT NUMBER**

**6. AUTHOR(S)**

Scott A. Trammell
Brett Martin

**5d. PROJECT NUMBER**

**5e. TASK NUMBER**

**5f. WORK UNIT NUMBER**

**7. PERFORMING ORGANIZATION NAME(S) AND ADDRESS(ES)**

Center for Bio/Molecular Science and Engineering
Code 6900
Naval Research Laboratory
Washington, DC 20375

**8. PERFORMING ORGANIZATION REPORT NUMBER**

**9. SPONSORING / MONITORING AGENCY NAME(S) AND ADDRESS(ES)**

Defense Threat Reduction Agency
8725 John J. Kingman Road STOP 6201
Fort Belvoir, VA 22060
PM/Calvin Shipbaugh

**10. SPONSOR/MONITOR'S ACRONYM(S)**
DTRA

**11. SPONSOR/MONITOR'S REPORT NUMBER(S)**
DTRA-TR-14-42

**12. DISTRIBUTION / AVAILABILITY STATEMENT**

Approved for public release; distribution is unlimited.

**13. SUPPLEMENTARY NOTES**

**14. ABSTRACT**

Reverse micelles (RMs) containing aqueous solutions of Ag+ ions in their core produce fluorescent Ag nanoclusters (NCs), upon exposure to gamma irradiation. The fluorescence spectra of the NCs evolves over days to weeks after the exposure, and usually show large increases in intensity. Responses of as high as 4 x 105 CPS/Gy were reached. A dosage of as low as 0.5 Gys (10% of the lethal dosage for humans) produces NCs having fluorescence intensities significantly higher than background. The RMs can be employed in novel gamma radiation detectors with appearance of fluorescence indicating that radiation was once present. In applications involving detection of fissile materials, the evolution of the fluorescence spectra over time may provide additional information about the radiation source. A two-phase liquid system is used for RM formation in a simple procedure. This synthesis method may be adapted to produce NCs from many other metal ions.

**15. SUBJECT TERMS**

reverse micelles, fluorescent silver nanocluster, radiation detection, gamma

| **16. SECURITY CLASSIFICATION OF:** | | | **17. LIMITATION OF ABSTRACT** | **18. NUMBER OF PAGES** | **19a. NAME OF RESPONSIBLE PERSON** |
|---|---|---|---|---|---|
| **a. REPORT** | **b. ABSTRACT** | **c. THIS PAGE** | UU | 25 | Calvin Shipbaugh |
| Unclassified | Unclassified | Unclassified | | | **19b. TELEPHONE NUMBER** *(include area code)* 703-767-3182 |

# CONVERSION TABLE

Conversion Factors for U.S. Customary to metric (SI) units of measurement.

| MULTIPLY → | BY → | TO GET |
|---|---|---|
| TO GET ← | BY ← | DIVIDE |

| | | |
|---|---|---|
| angstrom | 1.000 000 x E -10 | meters (m) |
| atmosphere (normal) | 1.013 25 x E +2 | kilo pascal (kPa) |
| bar | 1.000 000 x E +2 | kilo pascal (kPa) |
| barn | 1.000 000 x E -28 | meter$^2$ ($m^2$) |
| British thermal unit (thermochemical) | 1.054 350 x E +3 | joule (J) |
| calorie (thermochemical) | 4.184 000 | joule (J) |
| cal (thermochemical/$cm^2$) | 4.184 000 x E -2 | mega joule/$m^2$ ($MJ/m^2$) |
| curie | 3.700 000 x E +1 | *giga bacquerel (GBq) |
| degree (angle) | 1.745 329 x E -2 | radian (rad) |
| degree Fahrenheit | $t_k = (t^\circ f + 459.67)/1.8$ | degree kelvin (K) |
| electron volt | 1.602 19 x E -19 | joule (J) |
| erg | 1.000 000 x E -7 | joule (J) |
| erg/second | 1.000 000 x E -7 | watt (W) |
| foot | 3.048 000 x E -1 | meter (m) |
| foot-pound-force | 1.355 818 | joule (J) |
| gallon (U.S. liquid) | 3.785 412 x E -3 | meter$^3$ ($m^3$) |
| inch | 2.540 000 x E -2 | meter (m) |
| jerk | 1.000 000 x E +9 | joule (J) |
| joule/kilogram (J/kg) radiation dose absorbed | 1.000 000 | Gray (Gy) |
| kilotons | 4.183 | terajoules |
| kip (1000 lbf) | 4.448 222 x E +3 | newton (N) |
| kip/inch$^2$ (ksi) | 6.894 757 x E +3 | kilo pascal (kPa) |
| ktap | 1.000 000 x E +2 | newton-second/$m^2$ ($N-s/m^2$) |
| micron | 1.000 000 x E -6 | meter (m) |
| mil | 2.540 000 x E -5 | meter (m) |
| mile (international) | 1.609 344 x E +3 | meter (m) |
| ounce | 2.834 952 x E -2 | kilogram (kg) |
| pound-force (lbs avoirdupois) | 4.448 222 | newton (N) |
| pound-force inch | 1.129 848 x E -1 | newton-meter (N-m) |
| pound-force/inch | 1.751 268 x E +2 | newton/meter (N/m) |
| pound-force/foot$^2$ | 4.788 026 x E -2 | kilo pascal (kPa) |
| pound-force/inch$^2$ (psi) | 6.894 757 | kilo pascal (kPa) |
| pound-mass (lbm avoirdupois) | 4.535 924 x E -1 | kilogram (kg) |
| pound-mass-foot$^2$ (moment of inertia) | 4.214 011 x E -2 | kilogram-meter$^2$ ($kg-m^2$) |
| pound-mass/foot$^3$ | 1.601 846 x E +1 | kilogram-meter$^3$ ($kg/m^3$) |
| rad (radiation dose absorbed) | 1.000 000 x E -2 | **Gray (Gy) |
| roentgen | 2.579 760 x E -4 | coulomb/kilogram (C/kg) |
| shake | 1.000 000 x E -8 | second (s) |
| slug | 1.459 390 x E +1 | kilogram (kg) |
| torr (mm Hg, $0^0$ C) | 1.333 22 x E -1 | kilo pascal (kPa) |

*The bacquerel (Bq) is the SI unit of radioactivity; 1 Bq = 1 event/s.

**The Gray (GY) is the SI unit of absorbed radiation.

**Table of Contents**

**Executive Summary**

Reverse micelles (RMs) containing aqueous solutions of Ag+ ions in their core produce fluorescent Ag nanoclusters (NCs), upon exposure to gamma irradiation. The fluorescence spectra of the NCs evolves over days to weeks after the exposure, and usually show large increases in intensity. Responses of as high as 4 x 105 CPS/Gy were reached. A dosage of as low as 0.5 Gys (10% of the lethal dosage for humans) produces NCs having fluorescence intensities significantly higher than background. The RMs can be employed in novel gamma radiation detectors with appearance of fluorescence indicating that radiation was once present. In applications involving detection of fissile materials, the evolution of the fluorescence spectra over time may provide additional information about the radiation source. A two-phase liquid system is used for RM formation in a simple procedure. This synthesis method may be adapted to produce NCs from many other metal ions.

**Personnel Supported**

Scott A. Trammell

Brett D. Martin

**Collaborations**

Jake Fontana

Zheng Wang

James Louis-Jean

**Paper and Patients**

Generation of fluorescent silver nanoscale particles in reverse micelles using gamma irradiation. Brett D. Martin, Jake Fontana, Zheng Wang, James Louis-Jean , Scott A. Trammell, *Chem. Commun*. **2012**, 48, 10657-10659.

Synthesis of fluorescent silver nanoclusters in reverse micelles using gamma irradiation – low vs. high dosages and spectral evolution Brett D. Martin, Jake Fontana, Zheng Wang, and Scott A. Trammell *2013* Submitted to *Nanoscale*

Scott A. Trammell, Brett D. Martin, “Encapsulated Fluorescent Silver Nanoparticles as Novel Indicators for High-Energy Ionizing Radiation” U.S. Patent Application 61/647,702, May 16, 2012

**List of Figures and Tables**

## Introduction

Our objective for the project was to investigate the use of in-situ-formed fluorescent Ag nanoclusters (NCs) for detection of high-energy ionizing radiation such as gamma rays. Metal NCs are at a length scale between atoms and nanoparticles and often have desirable properties typical of large organic molecules (bright fluorescence, for example) since their band structure is broken down into discrete energy levels (1). NC synthesis can be challenging, however, because they tend to aggregate in solution to form larger particles. Thus, molecular stabilizers and "nanoscaffolds" are used to prevent this. The reduction of Ag ions in these systems is carried out chemically, photochemically or by radiolysis (2). In fact, both photochemical reduction and radiolysis have advantages since the addition of chemical reductants and subsequent purification is not needed (1, 3-5).

Radiolytic reduction methods that produce Ag NCs in bulk aqueous solutions are simple and reproducible, (2, 6) however, it appears that synthesis of fluorescent NCs via this means is not common. We described our work using silver ion-containing reverse micelles (RMs) to generate fluorescent silver nanoclusters (NCs) upon exposure to gamma irradiation. The $Ag^+$ was sequestered into the aqueous core of the RMs. In this system, gamma-ray exposure causes the water molecules contained in the core to undergo bond scission reactions, yielding solvated electrons, hydroxyl radicals, and hydrogen atoms (8). This process causes rapid reduction of the $Ag^+$ ions to $Ag^0$ atoms that aggregate into NCs that are often fluorescent. NC encapsulation in the RM prevents their further aggregation that would likely lead to loss of fluorescence.

**Fluorescent Metal NCs as Detectors of Fissile Isotopes** Our work had two goals. First, we wished to explore the use of the RMs as detectors of gamma radiation emitted by fissile materials. This is within the context of detection and tracking of radioactive isotopes used in weapons of mass destruction (WMD). Our second goal has been to develop this strategy as a general means for the synthesis of highly fluorescent Ag NCs, for any application. For both goals, the use of low energy gamma radiation in NC formation is highly desirable. For issues related to WMD, the ability to detect sub-lethal levels of radiation is very important. For humans, the threshold of lethality is about 5 Gys (9). Hence in our work described below we investigate the use of low gamma-ray dosage levels (0.5 – 5 Gys) for NC synthesis as well as initial studies using higher ones (up to 1000 Gys).

For applications in detection and tracking of WMD based on radioactive fissile isotopes, we envision that the RMs could be suspended in a transparent resin (such as varnish) that would then be applied to the insides of shipping containers, for example. Periodic testing for fluorescence will reveal if gamma radiation was once present. The intensity and spectral characteristics of the fluorescence, as well as the manner in which they evolve over time (hours to weeks after exposure) may allow the exact time of the exposure to be calculated. They may also permit the elemental identity of the emitting isotope(s) to be determined.

**Fluorescent NC Synthesis using Block Copolymer-Based Reverse Micelles**

In Figure 1, we show our strategy for Ag NC synthesis that uses RMs formed from block copolymers to confine the reactants in an aqueous core. The copolymers used are relatively short and have only two blocks, one composed of polyacrylic acid (PAA) and the second composed of polystyrene (PS). Block copolymers such as this display useful solution and associative properties when they are dissolved in solvents that can dissolve one block but not the other. One such associative structure is the RM (10).

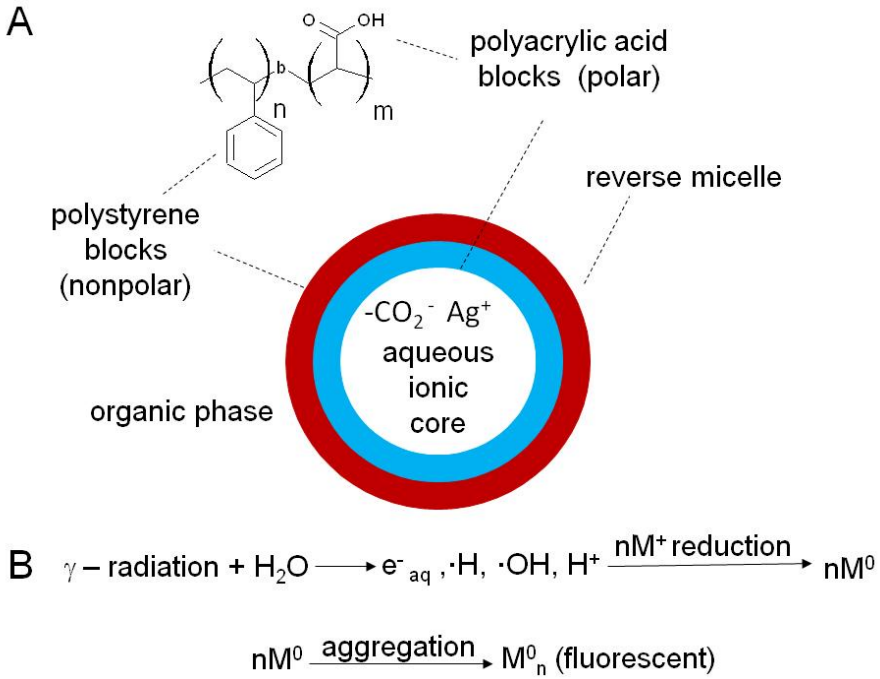


**Figure 1**. (A) PS-PAA block copolymer structure, and depiction of RM with aqueous ionic core having PAA carboxylate termini-$Ag^+$ ion pairs; (B) radiolysis reactions: $e^-_{aq}$ = solvated electron; $M^0$ = $Ag^0$; $Mn^0$ = Ag NC. Reproduced from (7).

Advantages of the PS-PAA RM system include low critical micelle concentrations (11), a well-characterized water-solvent solubility equilibria (12), and some understanding of the scaling relationships between the size of the ionic blocks and metal ions for the formation of metal nanoparticles (13-16). The aqueous core contains the Ag+ and the AA carboxylate residues which may be, to a large extent, ion-paired since the morpholine sulfonic acid (MOPS) buffer maintains the pH at 7.2, higher than the pKa of the acrylic acid residues, which is ~4.5. When gamma radiation interacts with the core, solvated electrons and radical species (such as hydroxyl radicals) are generated as shown in Figure 1B. In our system, the most likely reductant for the $Ag^+$ is the solvated electron. When aqueous solutions are irradiated at neutral and basic pH, it is the predominant reducing species (11). The solvated electron produces $Ag^0$ from Ag+ and the

atoms will then associate to form Ag NCs, a process that may be influenced by the spacing of the PAA repeat units.

**Methods**

Materials Reagents were obtained as follows and used without further purification: 3-(N-morpholino) propanesulfonic acid (MOPS), $AgNO_3$, and spectroscopic grade toluene were purchased from Sigma-Aldrich (St Louis, MO). The PS-PAA block co-polymers were purchased from Polymer Source Inc. (Quebec, Canada).

**Formation of RMs** In a typical two-phase synthesis of reverse micelles containing an aqueous core, commercially available PS-PAA having a polystyrene block and a polyacrylic acid block was dissolved at a concentration of 2 mg/mL in 10 mL toluene. The solution was placed into a 20 ml vial. A 10 mM morpholine sulfonic acid (MOPS) buffer (pH 7.2) was prepared and silver nitrate was added in the appropriate amount in the dark to form a 10 mM solution. The solution was shielded from light. Next, 10 mL of this aqueous solution was added to the toluene solution, a stir bar was placed in the vial, the vial was shielded from light and stirred at 30 RPM for either 16 hrs or 72 hrs at room temperature. Afterwards, the stirring was stopped and one mL aliquots were then removed from the toluene phase, which was the top phase. The aliquots were aerated (they were not sparged to remove dissolved $O_2$).

**Radiation** Most of the aliquots were subjected to gamma irradiation from a $^{60}Co$ source for various time durations, and the total doses were recorded. Other aliquots were not irradiated and used for control experiments. Irradiation experiments were performed using a $^{60}Co$ source at the Naval Research Laboratory (Washington, DC). Samples were irradiated at dosage rates ranging from 0.5 Gy/min to 508 Gy/min. Samples were stored in the dark after irradiation. Experiments were performed in triplicate.

**Characterization** The set of aliquots were characterized using UV-visible and fluorescence spectrometry, and TEM imagery and analysis. UV-visible measurements were made with an Agilent 8453 diode array spectrometer and referenced against a solvent blank. Fluorescence measurements were made with a Fluoromax-3 (Horiba) fluorimeter, using a bandpass of 5 nm for the excitation and emission monochromators with integration set at 0.1 s. Emission spectra were corrected using correction factors supplied by the manufacturer. For spectroscopy, 1 mL fluorescence quartz cuvettes were used. TEM imagery was performed using a JEOL JEM-2200FS field emission electron microscope. An SPI 200 holey carbon mesh was coated on a Cu TEM grid, which was placed onto a Teflon sheet in a fume hood. Three 5 microliter droplets of toluene containing the Ag NCs were placed onto the grid at 60 second intervals, allowing for the toluene to evaporate between each drop. Thermogravimetric analysis (TGA), and voltammetric stripping were performed using a Thermogravimetric Analyzer (Model 2950, TA Instruments, New Castle, DE), and a CH Instruments (Austin, TX) Model 700D potentiostat, respectively.

## Results and Discussion

**NC Formation at High Dosages** In our initial studies using the dosage range 2 Gys – 1000 Gys, we characterized the NCs using UV-visible/fluorescence spectroscopy and dose responses (fluorescence intensity (CPS, or photon counts per second) divided by dosage (Gys)), which allowed us to make a final selection of the optimal copolymer PAA block size. We also determined the initial $Ag^+$ and copolymer concentration in the liquid phase used for RM formation (toluene), and the $Ag^+$ consumption rates in the RMs as a function of dosage. These results will be discussed in detail below.

We used commercially available PS-PAA copolymers having different ratios of PS and PAA, dissolved in toluene. Encapsulation of $Ag^+$ ions into the aqueous core was accomplished by using a two phase system with the polymer-toluene solution on the top, and the buffer on the bottom (pH 7.2, 10 mM MOPS) containing $AgNO_3$. In these initial studies, the two phases were allowed to remain in contact for 16 hrs. To generate the fluorescent Ag NCs, 1 mL aliquots of the toluene layer were irradiated in a $^{60}Co$ pool at various doses. The toluene solutions that had not been irradiated showed no peaks in the visible absorbance spectra.

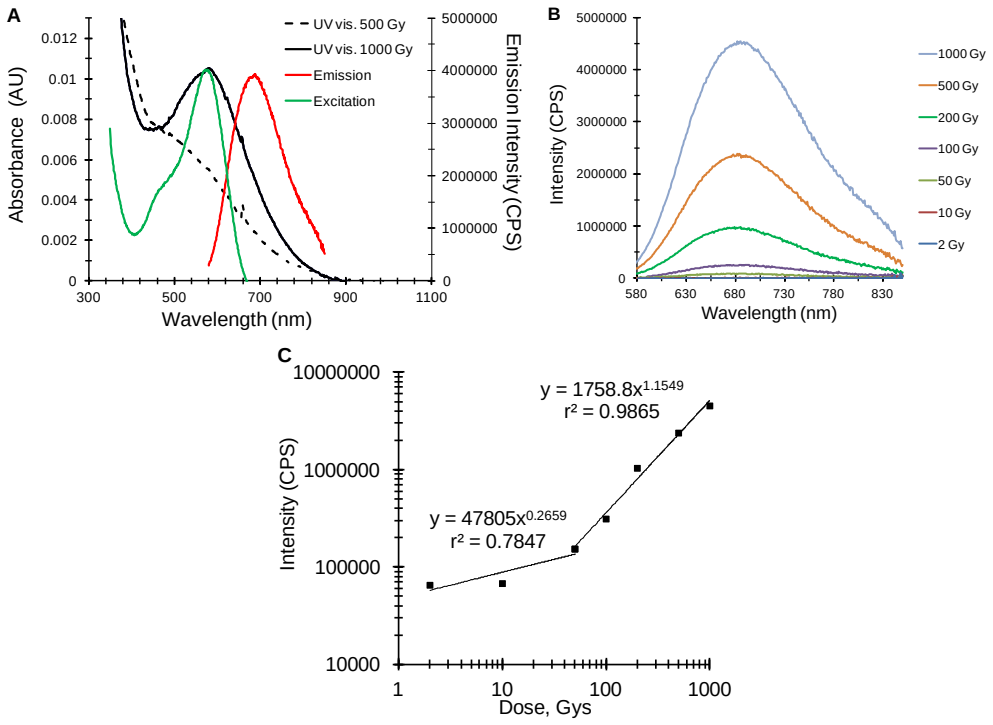


**Figure 2**. A) UV-visible, emission, and excitation spectra for 1000 Gy exposure; UV-visible spectra for 500 Gy exposure (reproduced from (7)). B) Emission spectra as a function of dosage. C) Peak emission intensity as a function of dosage.

Samples exposed to gamma irradiation in the dosage range 200 Gys - 1000 Gys showed a broad UV-visible absorption peak centered at 565 nm, which we presumed arose from the Ag NCs

(Figure 2A). The results were consistent with literature reviews reporting that photoreductive methods with a PAA terpolymer template gave metal NCs with an absorbance centered at ~ 500 nm (4). Other reviews indicated that Ag NCs formed in acrylates in general give a single emission band centered in the region from ~550 nm to 650 nm. Excitation at 565 nm (Figure 2A) generates a NC fluorescence spectrum with a broad emission maximum centered at 690 nm (Figures 2A, 2B). Several other samples were subjected to a progression of lower doses (500 Gys, 200 Gys, 100 Gys, 50 Gys, 10 Gys, and 2 Gys) and the spectra are given in Figure 2B. The same type of broad emission peak is seen for each case, with the maxima occurring in the range 670 nm - 690 nm. From the samples generated with a dose of 1000 Gy, we estimated the fluorescent quantum yield of the Ag NC to be ~ 4.7 %. Control experiments with samples that were not irradiated, or solutions irradiated with no $Ag^+$ show negligible fluorescence emission between 600 and 850 nm.

Figures 2B-C show that the peak fluorescence intensities have a linear dependence on dosage levels that can be broken into two linear, or quasi-linear, fits, as shown in Figure 2C. The weak dosage-fluorescence intensity relation in the low range led us to explore different approaches for the detection of low doses, in the range 0.5 to 5.0 Gys, as described below. Before investigating low dosage detection, we first wished to answer three questions - 1) how does the type of block copolymer used in RM formation ultimately affect the NC fluorescence?, and 2) what is the mass composition of the RMs immediately after formation (in terms of the amounts of $Ag^+$ and block copolymer present)? , and 3) how does the consumption rate of the $Ag^+$ depend on dosage level?

To address the first question, using a set of commercially available PS-PAA block copolymers we studied the manner in which the block lengths ultimately affected the fluorescence of the NCs. We used a 1000 Gy dosage in each case. The results were expressed in terms of response to dosage (peak fluorescence intensity divided by dosage) (Table 1).

**Table 1**. Block copolymers and dose responses.

| Polymer # | PS, MW | PAA, MW | Total MW | Response |
|---|---|---|---|---|
| 1 | 11000 | 300 | 11300 | 71 |
| 2 | 12000 | 1100 | 13100 | 206 |
| 3 | 1900 | 1400 | 20400 | 196 |
| 4 | 15000 | 3600 | 18600 | 341 |
| 5 | 42000 | 4500 | 46500 | 2264 |
| 6 | 5000 | 4800 | 9800 | 3042 |

[a] Response = fluorescence intensity (photon counts per second, cps/dose (Gy))

Table 1 lists the various polymers tested. When plotting the MW of the PAA block vs. dosage response (the amounts of polymer and $AgNO_3$ were held constant) we found that the response increased significantly at a MW threshold between 3600 and 4800 (Figure 3). Polymer 6 gave the greatest response, with its PAA block having a MW of 4800. The block copolymer yielding NCs with the highest response had roughly equal lengths of PS and PAA, which may enable it to form especially stable RMs.

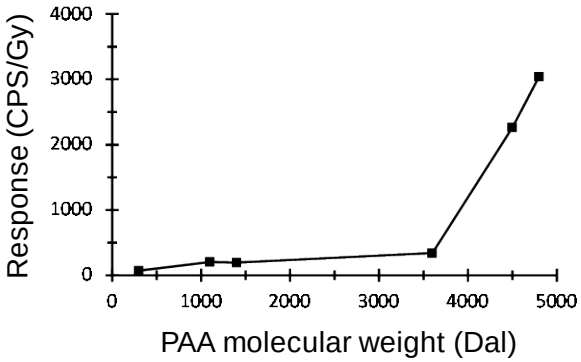


**Figure 3**. For the set of copolymers examined, response (CPS/Gy) as a function of the PAA coblock MW. Error bars are ± 4%.

To address the second question posed above, we formed the RMs using Polymer 6 in toluene, using our standard procedure. The amounts of polymer and $Ag^+$ were then found using thermogravimetric analysis (TGA) and anodic stripping square wave voltammetry (ASSWV). In the toluene phase we found that the $Ag^+$ and the polymer were present at levels of 0.061 mg/ml ± 6% (0.57 mM), and 0.57 mg/ml ± 6% (0.057 mM), respectively (7). Thus, the mass of the $Ag^+$ was 10-fold lower than that of the polymer, but the molar concentration of the $Ag^+$ was 10-fold higher than that of the polymer. This suggested that the PAA portion of each block copolymer molecule in the RM was ion-paired with 10 $Ag^+$ ions.

To address the third question posed above, using both irradiated and non-irradiated samples we extracted the $Ag^+$ ions from the RM-toluene solution into buffer. We then performed ASSWV and calculated the amount of $Ag^+$ that had reacted (7). Interestingly, we found that the highest $Ag^+$ consumption rates occurred at the lowest dose of 50 Gys (Figure 4). However, only relatively weak fluorescence appears at 50 Gys (Figures 2B-C). Evidently, at that dosage a large population of Ag NCs is formed, with 1) all having weak fluorescence that may change over time, or 2) some having weak fluorescence that may change over time but others being pre-fluorescent or permanently non-fluorescent. A final key question emerged – how does the spectral evolution of the weakly fluorescent and pre-fluorescent species occur over time?

This gave us added incentive to explore how low gamma doses, combined with post-exposure time-dependent spectral analysis, and ways of treating the RMs post-exposure could ensure maximum, or the most efficient, transformation of the weakly- and pre-fluorescent species into

bright fluorescent ones. Our goal was to use low doses of 0.5 to 5 Gys to achieve fluorescence intensities equal to those attained from exposure to several hundred Gys or higher in our previous work. As mentioned in the Introduction, this may ultimately allow development of gamma radiation detectors with much higher sensitivities, and allow development of synthesis methods for fluorescent NCs that will require much lower irradiation energies.

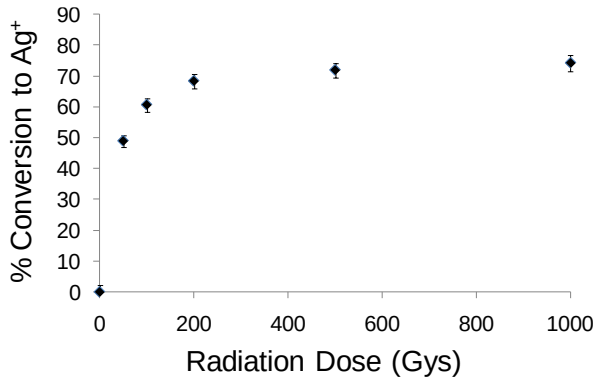


**Figure 4**. Conversion of $Ag^+$ as a function of gamma dosage, as determined using ASSWV (reproduced from (7)).

**NC Formation at Low Dosages - Time-Dependent Spectral Evolution and TEM Imagery**

Before we proceeded with the low-dosage studies, we decided to investigate whether the RM formation process and ultimately NC fluorescence could be affected by using a longer equilibration time for the two liquid phases (toluene and buffer). Interestingly, when the equilibration time was increased from 16 hrs to 72 hrs, pronounced dose-dependent effects on fluorescence intensity resulted. Dosages of 2 Gys and 50 Gys were examined, using an excitation maxima of 565 nm. For the 2 Gy dosage, the 72 hr equilibration time led to a substantially higher fluorescence intensity than the 16 hr time (Figure 5A), which yielded levels near zero (the background spectra were subtracted). However, for the 50 Gy dosage the 16 hr equilibration time was optimal, leading to a peak intensity that was ~20% higher than that attained from the 72 hr time (Figure 5B). Thus, longer equilibration times appear best for lower dosages whereas shorter times appear best for higher dosages. The mass transfer that occurs across the liquid-liquid phase boundary is probably a dynamic process involving time-dependent formation of RM populations having variable sizes and contents. The relationship between RM formation, dosage, and NC development is an attractive area for further investigation.

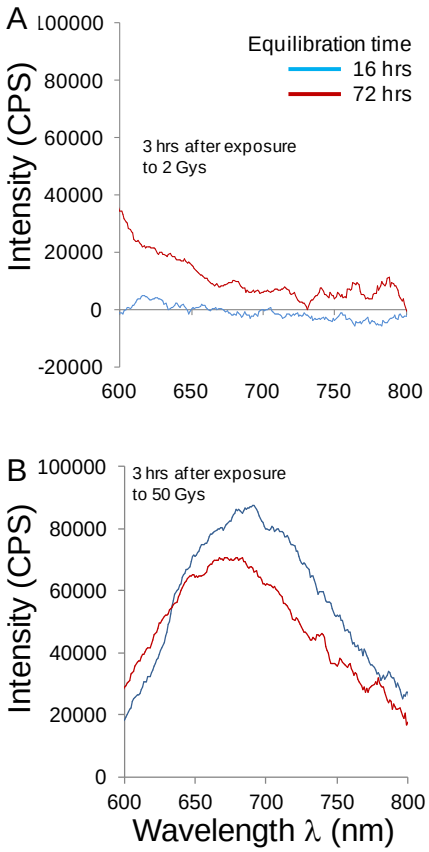


**Figure 5A-B**. NC emission intensity as a function of the 2-phase equilibration times and dosage levels (A, 2 Gys; B, 50 Gys).

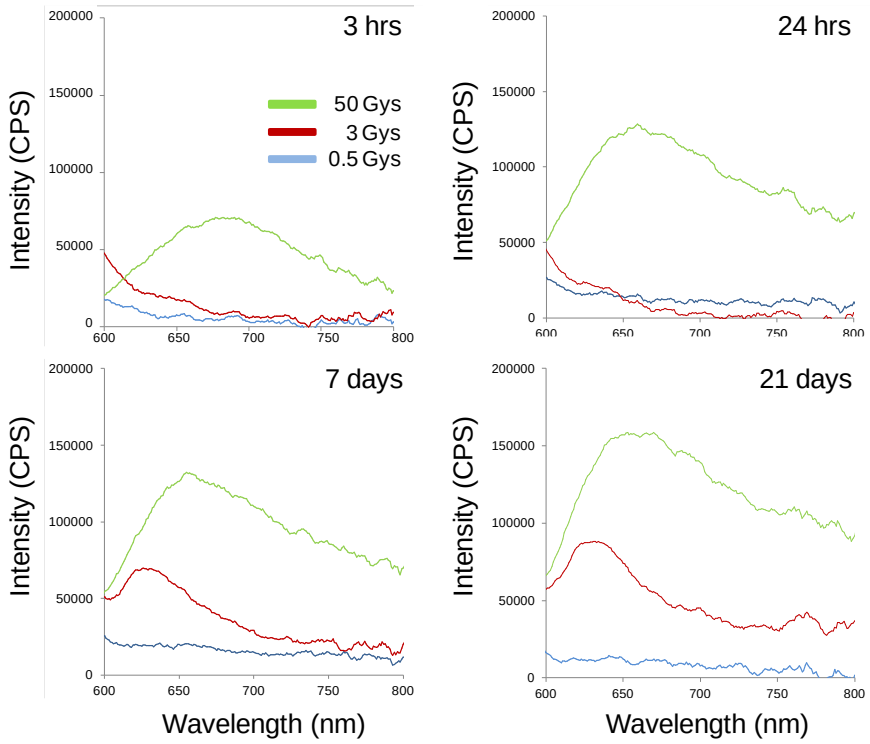


**Figure 6**. Dosage and time-dependent spectral evolution of the NCs from 3 hrs to 21 days after exposure.

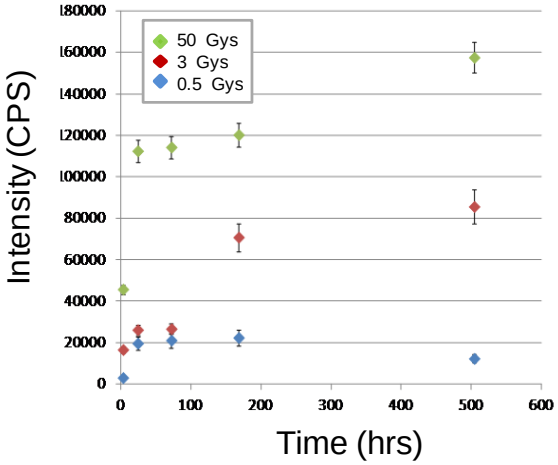


**Figure 7**. Dosage and time-dependent intensity of emission at $\lambda_{max}$, from 3 hrs to 21 days after exposure.

For the next set of studies using the lower dosage range 0.5Gys – 50 Gys, the RMs were formed using the standard two-phase system, with the 72 hr equilibration time. The samples were exposed to gamma irradiation in the same manner as before.

Their resulting UV-visible absorption spectra showed very low absorptivities, and are not shown. However, the NC fluorescence spectra showed significant dose-dependent differences (excitation maximum @ 565 nm) and changed gradually over hours and days after exposure (Figure 6). The spectra from samples that were not exposed to radiation (background spectra) have been subtracted from each. Several phenomena are apparent from the time course. First, the relatively very low dose of 0.5 Gys is sufficient to cause formation of fluorescent NCs. However, they do not have well-defined emission maxima, and there is no significant spectral change over time. For the higher dose of 3 Gys, the early spectra are similar to those for the 0.5 Gy exposure over the first few days. However, at t = 7 days an emission maximum at 630 nm appears. This may indicate that the NC size distribution may have narrowed to favor a certain size range. Over longer times up to 21 days, the fluorescence intensity increases slightly. For the highest dose of 50 Gys, the emission maximum at 680 nm appears at 3 hrs after exposure. Over the 21 day time course the fluorescence intensity increases, and the position of the emission maximum becomes blue-shifted to 655 nm. Figure 7 shows the time dependent emission intensity at the wavelength of maximum emission. For the 3 Gy and 50 Gy exposures, a dramatic increase in intensity appears at a distinct point in the time course with the increase for the higher dose occurring sooner.

The data in Figures 6 and 7 reveal that the NC formation processes are temporally dynamic. Properties such as average size and fluorescence intensity (ultimately quantum yield) are dependent on processes that are time-dependent. The fluorescence intensity undergoes conspicuous step-like changes that are in conjunction with long time periods with little apparent change. Examples of processes that may underlie these changes are rates of silver atom aggregation/deaggregation, rates of cluster aggregation/deaggregation, and diffusion rates of atoms and clusters.

Figure 8A-B shows TEM images of NCs formed at the various doses. They were imaged at 21 days after formation. For comparison, NCs that formed spontaneously without exposure to irradiation are shown also. Those formed in this manner have negligible levels of fluorescence. The NCs that formed without exposure have a clear non-homogeneous size distribution ranging from 2-3 nm to ~ 15 nm. In contrast, those formed via gamma-ray exposure have highly uniform size distributions, in the range 8-10 nm. It is of interest that there is virtually no variation in NC size as a function of dosage in the range 0.5 Gys to 50 Gys. However, comparison at higher magnification (Figure 8B) shows that the 3 Gy and the 50 Gy NCs are structurally more similar to one another than to the 0.5 Gy NCs. Finally, close examination of the NCs in Figure 8B reveals that they appear to be a conglomerate of smaller NCs. This is especially apparent for the NCs formed using 3 and 50 Gys.

It is also of interest that the background region appears to have a structure of its own, most readily seen in the images having a higher magnification. This structure was not visible when samples not having the block copolymer were imaged. The structure may in fact be the block

copolymer adsorbed onto the silicon surface, made visible in TEM by residual $Ag^+$ that is ion-paired to the PAA repeat units.

The findings depicted in Figures 6-8 can be summarized as follows. The NC size range attained via the 0.5 Gy dosage nearly matches the size range arising from the 3 and 50 Gy dosage, but in the latter two cases 1) the fluorescence intensity is ~8 and 16-fold higher, respectively, 2) a pronounced emission maxima becomes present, 3) the fluorescence intensity gradually increases over time, 4) a close structural similarity is seen, 5) they appear to be a conglomerate of smaller NCs. The NCs formed using the dose range 3 to 50 Gys are, evidently, profoundly different from those formed using a 0.5 Gy dosage. It may simply be that the low dosage does not generate enough solvated electrons through water scission, and the $Ag^+$ enters other chemical pathways that lead to formation of NCs with less desirable characteristics.

**Comparison of NCs Formed Using Low vs. High Dosages - Full-Spectrum Excitation and Emission Scans**

In a final study, we used a sample of RMs in toluene that had been exposed to a 5 Gy dosage. Here, we allowed 50% of the toluene to evaporate slowly at room temperature over a period of 14 days through a perforated cap. This caused the RMs to become concentrated by a factor of two. We then reconstituted the solution by adding enough solvent to return the RMs to their original concentration.

We then performed a fluorescence study in which we determined the manner in which the emission varied as a function of excitation $\lambda_{max}$ through the range 525 nm – 595 nm. The emission was measured by scanning through the range 610 nm to 700 nm. The resulting fluorescence spectra are shown in Figure 9A, with the chosen excitation $\lambda_{max}$ values tabulated in the legend. We then performed the analogous study wherein the monitored emission wavelength was chosen to be at various points in the range 610 nm – 700 nm, while the excitation wavelength was varied continuously through the range 400 nm – 670 nm (Figure 9B). The spectra from samples that were not exposed to radiation (background spectra) have been subtracted from each. In Figure 9A, two main results are immediately apparent. First, the fluorescence intensity at 565 nm excitation has increased by a factor of ~15 vs. the 3 Gy sample with its spectral data shown in Figures 6 and 7. The dramatic increase in fluorescence intensity evidently arises because the sample was concentrated 2-fold over the 14-day time course. The second important finding is that all of the spectra have a considerable amount of structure, i.e. they all have three relative maxima at 611-613 nm, 640-648 nm, and 705-709 nm. As the excitation wavelength is increased from 525 nm to 595 nm, the fluorescence intensity rises, then falls, then rises again. In Figure 9B, the spectra show even more structure, with all showing four relative maxima occurring at 517-522 nm, 558-559 nm, 591-595 nm, and 630-636 nm. The fluorescence intensity rises, then falls as the monitored emission wavelength is increased from 610 nm to 700 nm.

TEM imagery showed that the NCs formed using 3 and 50 Gys appear to be a conglomerate of smaller NCs. Each relative maxima seen in both fluorescence plots may represent a particular NC size, or narrow size distribution, present in the conglomerate. Thus, four discrete NC sizes/size distributions may be present.

As noted above, the NC fluorescence intensity increased by a factor of ~15 simply by allowing the RMs to concentrate by a factor of two in the toluene solvent. The underlying mechanism for this increase is not known at present, but further studies on concentration effects may allow a greater understanding of the exact chemical pathways that lead to formation of these types of NCs.

For comparison to the low-dosage spectra given in Figures 9A -B, we performed the same types of spectral experiments using samples formed from exposure to 1000 Gys. In this case the study was done 3 hrs after the 1000 Gy dosage, and the samples were not concentrated. So, the synthesis conditions differed as follows – 1000 Gy vs. 5 Gy dosage, spectra measured at 3 hrs vs. 14 days post-exposure, and no sample concentration vs. concentration by a factor of two. The spectra from the 1000 Gy exposure are seen in Figures 10A-B. Figure 10A gives the emission spectra that resulted when the excitation frequency was varied. It is qualitatively similar to Figure 9A, for the 5 Gy dose, except that the spectra are much smoother (unstructured) with only one relative maximum. We then performed the analogous study wherein

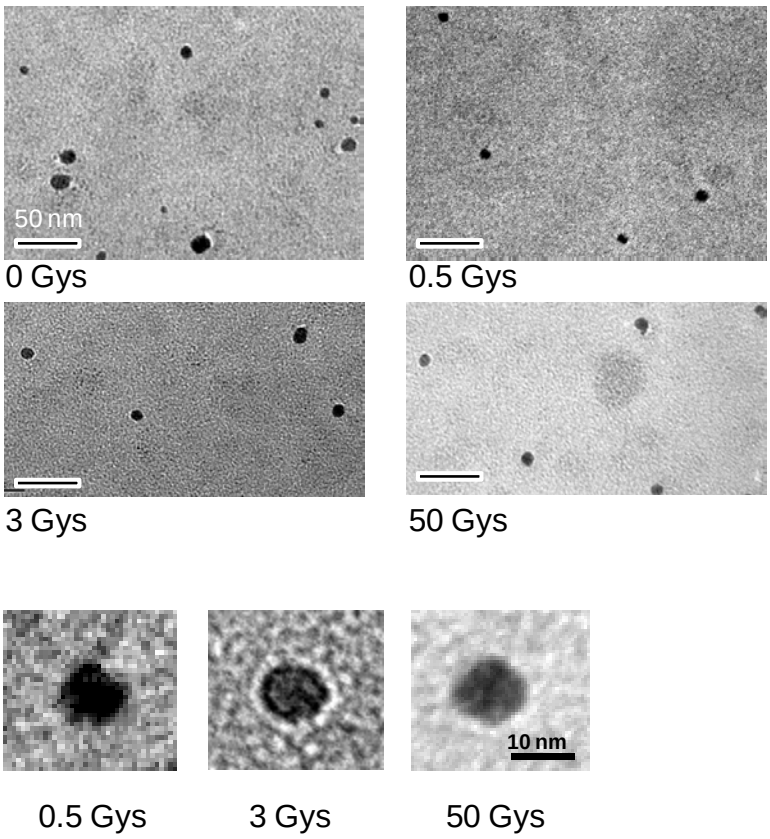


**Figure 8**. TEM images of Ag NCs formed at various gamma -ray dosages, and control (0 Gys).

the excitation wavelength was varied continuously over the range 400 nm – 675 nm, with the emission being monitored at points in the range 600 nm – 700 nm (Figure 10B). Again, the spectra are qualitatively similar to Figure 9B for the 5 Gy dose, but are much smoother with only one emission maximum. For the samples exposed to the 1000 Gy dosage, the excitation and emission spectra show a wavelength dependence that is typical of systems that display inhomogeneous broadening and have recently been reported for Ag NCs generated photochemically in DMF [17]. The lack of multiple relative maxima and associated structure may indicate that there is a much broader NC size distribution, with no set of discrete NC sizes. In an earlier study we found that NCs formed using 1000 Gy dosages were relatively large (~20 nm diameter) and were thought to contain "islands" of smaller fluorescent clusters in a non-fluorescent matrix[7].

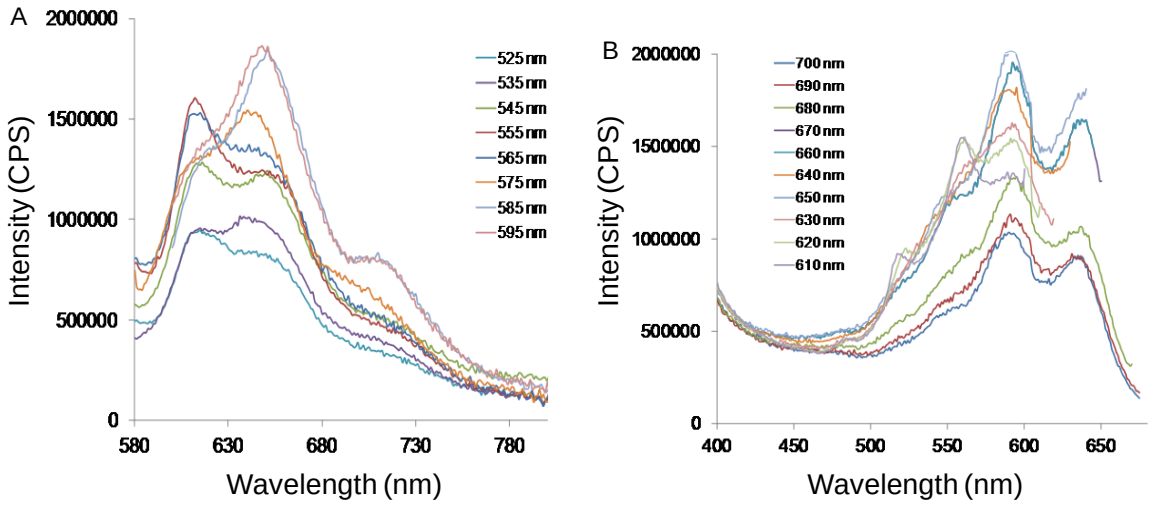


**Figure 9A-B**. Fluorescence emission (A) and excitation (B) spectra at 14 days after exposure to 5 Gys. In 9A, the legend denotes excitation $\lambda_{max}$; in 9B, the legend gives the emission wavelength monitored.

It is of interest that the 1000 Gy dosage gives ~4-fold higher fluorescence intensities than the 5 Gy dosage. However, the response (intensity/dose) for the 5 Gy dosage is much higher. It ranges from 2 x $10^5$ to 4 x $10^5$ CPS/Gy, whereas the response for the 1000 Gy dosage ranges from 4 x $10^3$ to 8.5 x $10^3$ CPS/Gy. Thus, the response for the 5 Gy dosage is ~30 to 40-fold higherthan that of the 1000 Gy dosage.

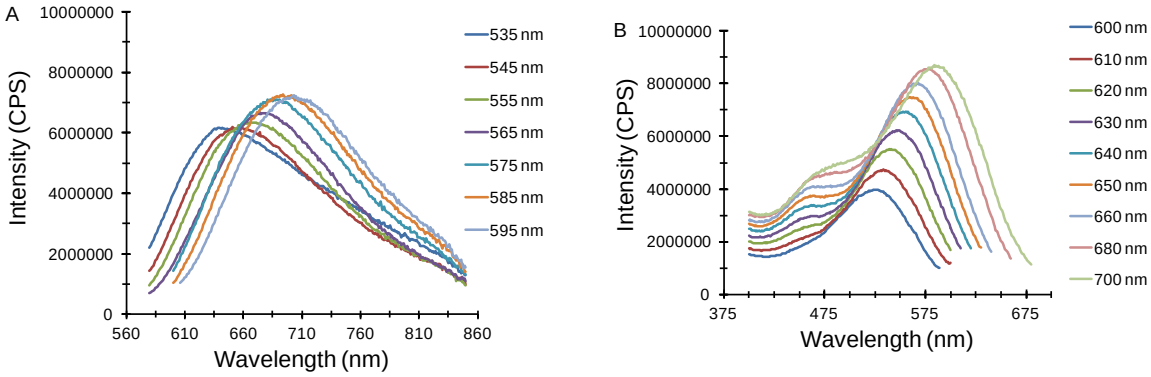


**Figure 10A-B**. Fluorescence emission (A) and excitation (B) spectra at 3 hrs after exposure to 1000 Gys. In 10A, the legend denotes excitation $\lambda_{max}$; in 10B, the legend gives the emission wavelength monitored.

The results from these studies are summarized in Table 2. Clearly, the NCs with the highest response are those that were permitted to age over long periods of time (weeks) while slowly concentrating in solution. Thus we have shown that Ag NCs with a high response can be formed using low, sub-lethal gamma-ray dosages in the range 0.5 to 5 Gys. In future work for the present

application, as well as others, one important possibility is the use of the RMs to form NCs that are composed of other metals (Au, Cu, Co, etc.) or their combinations, with or without Ag. These may represent an entirely new class of fluorophores and catalysts having unique properties.

**Table 2**. NC sample history and results

| Sample history | Dose (Gys) | Response (CPS/Gy) | Fluorescence Spectra |
|---|---|---|---|
| Tested at 3 hrs[1], 16 hr PET[2] | 1000 | $4 \times 10^3$ to $8.5 \times 10^3$ | broad $\lambda_{max}$ |
| Tested at intervals over 21 days[1], 72 hr PET | 0.5<br>3<br>50 | $4 \times 10^4$<br>$2.8 \times 10^4$<br>$3.2 \times 10^3$ | no $\lambda_{max}$ (0.5 Gy); $\lambda_{max}$ at later t (3 Gy); broad $\lambda_{max}$, all t (50 Gy) |
| Tested at 14 days[1], sample solution concentrated by a factor of 2, 72 hr PET | 5 | $2 \times 10^5$ to $4 \times 10^5$ | multiple relative maxima |

[1]after exposure; [2] phase equilibration time

**Conclusions**

Seven main conclusions can be drawn from our work presented here, which can be summarized as follows:

In initial studies using the dosage range 2-1000 Gys, fluorescence measurements 3 hrs after exposure show linear relations between emission intensity and dosage, with emission maxima occurring in the range 670 nm - 690 nm. A 16 hr phase equilibration time was used.

The block copolymer leading to NCs with the highest response (3042 CPS/Gy @ 1000 Gys) had roughly equal lengths of PS and PAA, which may enable it to form especially stable RMs.

RM mass composition studies 1) suggest that the PAA portion of each block copolymer molecule in the RM is ion-paired with 10 $Ag^+$ ions, and 2) show that the highest Ag+ consumption rate occurs at lower dosages.

In RM formation for lower dosages (2 Gys), longer equilibration times (72 hrs) lead to NCs having the most intense fluorescence. However, in RM formation for higher dosages (50 Gys), shorter equilibration times (16 hrs) lead to NCs having the most intense fluorescence.

The fluorescence intensity of NCs formed using dosages of 0.5 to 50 Gys evolves over a 21-day time period. Dosages of 3 and 50 Gys result in intensities and emission maxima that generally increase over this time. The maxima undergo conspicuous step-like changes that are in conjunction with long time periods with little apparent change.

TEM imagery shows that dosages of 3 and 50 Gys lead to NCs having a very narrow size distribution, with diameters of 8-10 nm. A close structural similarity is seen, and they appear to be a conglomerate of smaller NCs.

The NCs having the highest response (fluorescence/dosage) are those that were permitted to age over a period of time (2 weeks) while slowly concentrating in solution. Their response was in the range from $2 \times 10^5$ to $4 \times 10^5$ CPS/Gy.

**References**


1) I. Diez and R. H. A. Ras, Nanoscale, 2011, 3, 1963–1970.

2) H. X. Xu and K. S. Suslick, Adv. Mater., 2010, 22, 1078–1082.

3) J. G. Zhang, S. Q. Xu and E. Kumacheva, Adv. Mater., 2005,17, 2336.

4) J. Belloni, M. Mostafavi, H. Remita, J. L. Marignier and M. O. Delcourt, New J. Chem., 1998, 22, 1239–1255.

5) H. Zhang, X. Huang, L. Li, G. Zhang, I. Hussain, Z. Li and B. Tan, Chem. Commun., 2012, 48, 567.

6) J. Belloni, M. Mostafavi, H. Remita, J. L. Marignier and M. O. Delcourt, New J. Chem., 1998, 22, 1239–1255.

7) B. D. Martin, J. Fontana, Z. Wang, J. Louis-Jean, S. A. Trammell, Chem. Commun., 2012, 48, 10657–10659

8) R. J. Woods and A. K. Pikaev, Applied radiation chemistry: radiation processing, Wiley, 1994.

9) NRC Glossary (October 2011)

10) G. Riess, Prog. Polym. Sci., 2003, 28, 1107–1170.

11) M. Moffitt, K. Khougaz and A. Eisenberg, Acc. Chem. Res., 1996, 29, 95–102.

12) Z. S. Gao, A. Desjardins and A. Eisenberg, Macromolecules, 1992, 25, 1300–1303.

13) L. H. Bronstein, S. N. Sidorov, P. M. Valetsky, J. Hartmann, H. Colfen and M. Antonietti, Langmuir, 1999, 15,6256–6262.

14) I. W. Hamley, Nanotechnology, 2003, 14, R39–R54.

15) M. Moffitt, L. McMahon, V. Pessel and A. Eisenberg, Chem. Mater., 1995, 7, 1185–1192.

16) C. W. Wang and M. G. Moffitt, Langmuir, 2004, 20, 11784–11796.

17) I. Diez, R. H. A. Ras, M. I. Kanyuk and A. P. Demchenko, Phys.Chem. Chem. Phys., 2013, 15, 979-985

**DEPARTMENT OF DEFENSE**

DEFENSE THREAT REDUCTION
AGENCY
8725 JOHN J. KINGMAN ROAD
STOP 6201
FORT BELVOIR, VA 22060
ATTN: C. SHIPBAUGH

DEFENSE TECHNICAL
INFORMATION CENTER
8725 JOHN J. KINGMAN ROAD,
SUITE 0944
FT. BELVOIR, VA 22060-6201
ATTN: DTIC/OCA

**DEPARTMENT OF DEFENSE CONTRACTORS**

EXELIS, INC.
1680 TEXAS STREET, SE
KIRTLAND AFB, NM 87117-5669
ATTN: DTRIAC